

46p.

NASA TECHNICAL  
MEMORANDUM

N64-22480  
CODE-1 CAT. 31  
NASA TM X-53007

February 3, 1964

NASA TM X-53007

# **DESTRUCT TESTS ON SCALE MODEL SATURN I BOOSTER**

by J. B. GAYLE AND C. H. BLAKEWOOD

Propulsion and Vehicle Engineering Laboratory

NASA

*George C. Marshall  
Space Flight Center,  
Huntsville, Alabama*

OTS PRICE

XEROX

\$

4.60 ph

MICROFILM

\$

\_\_\_\_\_

NASA - GEORGE C. MARSHALL SPACE FLIGHT CENTER

---

TECHNICAL MEMORANDUM X-53007

---

DESTRUCT TESTS ON SCALE MODEL SATURN I BOOSTER

by

J. B. Gayle and C. H. Blakewood

ABSTRACT

22480

Multiple tank clusters representing Saturn I boosters and containing 3,500 pounds of LOX/RP-1 were destructed by using internal and external destruct systems. The explosive yields for both systems were low and, therefore, tended to refute the suggestion that the cluster configuration of this vehicle necessarily would result in increased yields by comparison with vehicles having dual tanks in tandem configuration. Comparisons of results for the two destruct systems indicated somewhat lower yields and less fragmentation for the external destruct system.

AUTHOR

NASA - GEORGE C. MARSHALL SPACE FLIGHT CENTER

---

TECHNICAL MEMORANDUM X-53007

---

DESTRUCT TESTS ON SCALE MODEL SATURN I BOOSTER

by

J. B. Gayle and C. H. Blakewood

MATERIALS DIVISION  
PROPULSION AND VEHICLE ENGINEERING LABORATORY

# TABLE OF CONTENTS

	Page
SUMMARY. . . . .	1
INTRODUCTION . . . . .	1
ACKNOWLEDGMENT . . . . .	2
TEST CONFIGURATIONS AND OPERATING PROCEDURES . . . . .	2
INSTRUMENTATION . . . . .	3
Shock Wave Measurements . . . . .	5
Shrapnel Measurements . . . . .	7
Fireball Measurements . . . . .	7
CALIBRATION OF INSTRUMENTATION . . . . .	7
RESULTS . . . . .	11
Fragmentation . . . . .	11
Fireball. . . . .	13
Shock Waves . . . . .	14
CONCLUSIONS. . . . .	15
REFERENCES . . . . .	38

# LIST OF TABLES

Table	Title	Page
I	Specifications for Test Configurations . . . .	4
II	Gauge and Camera Distances for Cluster Tests . . . . .	8
III	Sensitivity Coefficients for Piezoelectric Gauges . . . . .	10
IV	Approximate Temperature Profiles . . . . .	14
V	Number of Significant Explosions Indicated by Different Types of Instrumentation. . . . .	15

# LIST OF FIGURES

Figure		Page
1	Cluster in Place at Test Site . . . . .	17
2	Details of Destruct Systems . . . . .	18
3	Location of Destruct Systems. . . . .	19
4	Blast Instrumentation Layout . . . . .	20
5	Shock Tube Used for Calibration . . . . .	21
6	Oscilloscope Trace for Typical Shock Wave . . .	22
7	Calibration Data and Reference Curve for Piezoelectric Gauges. . . . .	23
8	Calibration Data and Reference Curve for Foilmeter Gauges. . . . .	24
9	Calibration Data and Reference Curve for Cantilever Beam Gauges. . . . .	25
10	Calibration Data for Self-Record Gauges . . . .	26
11	Time of Arrival of Shock Wave As Measured with Fastax Camera. . . . .	27
12	Fragment Pattern for Single LOX Container, Test S-1. . . . .	28
13	Fragment Pattern for Single Fuel Container, Test S-2. . . . .	29
14	Fragment Pattern for Test C-1 (External Destruct System). . . . .	30
15	Fragment Pattern for Test C-2 (External Destruct System). . . . .	31
16	Fragment Pattern for Test C-3 (External Destruct System). . . . .	32
17	Fireball Size and Duration for Cluster Tests. .	33
18	Cantilever Beam Data for Cluster Tests. . . . .	34

LIST OF FIGURES (Concluded)

Figure		Page
19	Equivalent TNT Yield for Test C-1 (External Destruct System). . . . .	35
20	Equivalent TNT Yield for Test C-2 (External Destruct System). . . . .	36
21	Equivalent TNT Yield for Test C-3 (Internal Destruct System). . . . .	37

## DESTRUCT TESTS ON SCALE MODEL SATURN I BOOSTER

by

J. B. Gayle and C. H. Blakewood

22480

### SUMMARY

Multiple tank clusters representing Saturn I boosters and containing 3,500 pounds of LOX/RP-1 were destructed by using internal and external destruct systems. The explosive yields for both systems were low and, therefore, tended to refute the suggestion that the cluster configuration of this vehicle necessarily would result in increased yields by comparison with vehicles having dual tanks in tandem configuration. Comparisons of results for the two destruct systems indicated somewhat lower yields and less fragmentation for the external destruct system.

*author*

### INTRODUCTION

The explosive yield that results from the destruct of a launch vehicle is influenced by the design of the particular destruct system used.

An internal destruct system, consisting of Primacord enclosed in a well that was suspended in the propellant tanks, was used with the Redstone and Jupiter vehicles. Activation of this system caused a strong shock to be transmitted through the propellant to the tank walls which resulted in vehicle breakup and propellant dispersion. Ignition of the dispersed propellants took place instantaneously, thereby precluding appreciable mixing of the fuel and oxidizer and resulting in a negligible explosive yield.

The clustering of several fuel and oxidizer tanks in a side by side arrangement for the S-I stage of the Saturn I vehicle could be expected to increase greatly the rate and extent of mixing of the dispersed propellants, particularly with destruct systems of the internal type. An



experimental investigation, therefore, was initiated to determine the explosive yields resulting from destruct of the S-I stage with a conventional internal destruct system. Because a number of design considerations indicated that an external destruct system would afford distinct advantages in fabrication and installation, duplicate tests employing flexible linear-shaped charge (FLSC) taped to the outside of the tank walls were made.

#### ACKNOWLEDGMENT

The work on which this report is based was accomplished through the cooperation of the Materials Division, the Propulsion Division, and the Systems and Design Integration Division of the Propulsion and Vehicle Engineering Laboratory.

#### TEST CONFIGURATIONS AND OPERATING PROCEDURES

Two test configurations were used. Tests S-1 and S-2 used single tanks containing LOX and RP-1 which were destructed with FLSC to qualify the external destruct system. Tests C-1, C-2, and C-3 used nine-tank clusters containing a total of 3500 pounds of RP-1 and LOX in the usual ratio. Two of these tests used external FLSC destruct systems, and one used an internal Primacord system. FIG 1 is a photograph of a cluster in place at the test site; Table I is a summary of specifications for the tests.

All tanks were made of aluminum alloy Al-5456-H343 and consisted of right circular cylinders with hemispherical bulkheads. Skirts were attached at both ends of the tanks to provide means of assembly and to protect the bulkheads in handling. Each tank was provided with a fitting on the lower bulkhead for filling and another on the upper bulkhead for venting and pressurization. All LOX tanks were appropriately cleaned and degreased prior to use.

The external destruct system employed 100 grain/ft FLSC, having a Pentaerythritol tetranitrate core (PETN) in a shaped lead sheath taped against the tank walls (FIG 2a). On flight vehicles, the FLSC will be held away from the tank wall by an insulation sheath (FIG 2b) so that there is a  $0.094 \pm 0.015$  inch stand-off. The insulation is provided to protect against aerodynamic heating. The internal system employed 100 grain/ft Primacord, also with a PETN core, suspended in a 1.5-inch aluminum tube (FIG 2c). The aluminum tube was located three inches from the wall of each tank except the inner LOX tank, where a five inch spacing was allowed. Primacord (50 grain/ft) served as the fuse train from the detonator, which consisted of two M36A1 detonator caps.

For the single tank tests (S-1 and S-2), 40-inch lengths of FLSC were taped longitudinally to the cylindrical portions of the tanks. For the first cluster test (C-1), 40-inch lengths of FLSC were taped

to the outer tanks, and a 32-inch length was taped to the center tank facing an RP-1 container as shown in FIG 3a. For the second cluster test (C-2), 56-inch lengths of FLSC were taped longitudinally to the cylindrical portions and extended through the skirts onto the lower bulkheads of the outer tanks; also, 16-inch lengths of FLSC were attached to the skirts of these tanks in front of the extensions. No FLSC was attached to the cylindrical portion of the center tank, but two 36-inch lengths were taped to the lower bulkhead, thus, forming a cross as shown in FIG 3b. For the third cluster test (C-3), 49- and 29-inch lengths of Primacord were suspended in 1.5-inch diameter wells extending into the tanks as shown in FIG 3c.

Provision was made for explosively cutting and separating the main vent line at a distance of approximately seven feet from the clusters so that it could be reused with a minimum of repair. This entailed use of an additional 13 feet and 8 inches of 50 grain/ft Primacord and 3 feet and 6 inches 100 grain/ft FLSC for each test.

The procedure used for the single tank LOX test, S-1, consisted of mounting the tank on the stand and attaching the FLSC. The tank was filled with LOX and replenished after a ten minute waiting period. This allowed enough time for the countdown to proceed orderly before boil-off lowered the liquid surface to the proper level. The vent line then was closed, and the pressure was allowed to rise to the 43.5 psi vent pressure. At this time the destruct system was activated.

For the single tank RP-1 test, S-2, the FLSC was attached, then the tank was filled with RP-1 and pressurized to 17.5 psi with nitrogen from a cylinder. The tank valve was closed, (All tanks had been checked previously to determine that pressure could be maintained.) and the N<sub>2</sub> bottle was removed. The destruct system was then activated.

For the cluster tests, C-1, C-2, and C-3, the clusters were assembled on the stand, and the RP-1 tanks were filled. The instrumentation then was given a final checkout, and the destruct system was attached. Finally, the LOX tanks were filled; after the initial boil-off period, they were replenished, and the LOX supply was removed. The RP-1 tanks were pressurized and closed. Then the LOX tank vent valves were closed, and the destruct system was armed. LOX pressure was monitored continuously; when it reached 43.5 psi, the destruct system was activated.

## INSTRUMENTATION

Instrumentation was provided to obtain information regarding shock wave overpressures and velocities; fireball rates of growth, ultimate sizes, movements and temperatures; and shrapnel formation and dispersion.



## Shock Wave Measurements

The primary instrumentation used to measure shock wave overpressures resulting from the propellant detonations consisted of eleven piezo-electric pressure transducers, amplifiers, and a multi-channel FM tape recorder to record the gauge signals. The secondary system consisted of ten foil-meter or "Bikini" gauges, ten cantilever beam gauges, and three self-recording gauges. In addition, various cameras with framing rates ranging from 24 fps to 6,000 fps provided additional information and documentation of the tests. Temperature-sensitive paints were used to obtain information about temperatures in and near the fireballs.

The piezoelectric gauges were pencil type side-on pressure transducers mounted on blast insensitive stands approximately 24 inches above the ground surface and set at distances varying from 32 feet to 222 feet from the center of the explosion. Because of the limited dynamic range of the recorder and, consequently, the limited range of the overpressures readable by any particular gauge, and also because of the rapid decay of overpressure with distance, a constant logarithmic ratio was used to establish the spacing of individual gauges to provide valid data for one or more gauges for yields in the range of 10 to 3000 lbs of TNT. The locations of all gauges are shown in Figure 4 and Table II.

The output signal from each gauge was fed through six feet of coaxial cable inside the gauge mount to a unity gain preamplifier and line driver situated at the rear of the mount and encased in a protecting can. The amplifier output was connected to the tape recorder in the control bunker through approximately 1,100 feet of high impedance coaxial cable.

The tape recorder had twelve channels operating in the FM mode (20 kilocycle frequency response) and two channels operating in the Direct mode. Each gauge used one FM channel; a timing and calibration signal used one FM channel; voice identification used one Direct channel; the other Direct channel was not used. Recording speed was 60 inches per second (ips).

The calibration signal which served as a time reference for shock velocity and as a voltage reference for signal amplitude was a 1,000 cps sine wave of 3.0 volts peak-to-peak amplitude and was derived from a stable audio frequency oscillator. Calibration frequency and amplitude were monitored by a digital frequency meter and a calibrated oscilloscope.

The recorded signals from the transducers were played back at a reduced speed of 7-1/2 ips and were read out on a strip chart recorder operating at 40 ips. Then, the resulting records were measured on a digital chart reader to give signal amplitudes and times of arrival of signals at various gauges. Previously determined gauge calibration coefficients then allowed direct calculation of overpressures sensed by the gauges. The time of arrival data and the gauge spacings were used to compute shock velocity which in turn were used for indirect calculations of overpressures.

Subsequent to initial calibration tests but prior to test C-1, five of the preamplifiers sustained damage due to water penetration of the sealed protecting cans and were sent to the manufacturer for repair. Because they were not returned in time for the cluster tests, it was necessary to connect five of the piezoelectric gauges directly to the recorder. The resulting effects were a severe decrease in gauge time constant because of the relatively low input resistance of the recorder and a reduction in sensitivity because of the voltage divider action of the cable capacitance. Additional calibrations were made with this arrangement to obtain new sensitivity coefficients.

The range of overpressures which could be sensed for any particular gauge was determined by the point at which the recorder became distorted and by the signal to noise ratio of the system, including the readout instrumentation. Upper values were 1.8 volts peak, and lower values were approximately 10 millivolts peak. These voltages corresponded approximately to 10 psig and 0.05 psig, respectively, for the gauges with amplifiers and to 40 psig and 0.2 psig for the gauges without amplifiers.

Fastax camera coverage was provided to indicate time of arrival of the shock wave at various distances from the explosions. To facilitate data reduction, striped reference fences (FIG 4) were used to define the location of the shock wave, and millisecond timing marks on the edge of the film were used to estimate its velocity. These data also were used for indirect calculations of overpressures.

The three types of mechanical gauges, the foil-meter gauges, the cantilever beam gauges, and the self-recording gauges, were used primarily as a backup system for the piezoelectric gauges. The foil-meter and beam gauges were constructed in-house. Their characteristics are described in references 1, 2, and 3. The self-record gauges, described in reference 4, were obtained on loan from the Atlantic Missile Range.

All three types of these gauges are "self-recording" in that they are permanently and measurably altered or deformed by a shock wave. The foil-meters measure discrete ranges of overpressures by means of bursting diaphragms. The beam gauges measure a continuous range of overpressures by means of the permanent deformation of the aluminum beam. The self-recording gauges measure the entire pressure-time history of the shock wave by scribing a line whose deflection is proportional to the instantaneous overpressure on a rotating silvered glass disc.

While the first two types of mechanical gauges were completely inert, the self-recording gauges were driven by battery operated chronometric motors. These motors were initiated by an internal relay controlled by a 10 volt d.c. power supply in the control bunker. Approximately 15 seconds of recording time were available for each gauge without overlapping the beginning of the recording.

### Shrapnel Measurements

For observations on shrapnel, the area surrounding the test was surveyed after each test for fragments. The location, weight, and identification of each fragment were noted. The various film coverages provided the opportunity of observing the fragments in flight.

### Fireball Measurements

Temperature sensitive paints, "Tempilaq" were used to obtain rough estimates of temperatures near the edge of the fireball. A series of paints having critical temperatures that varied in 100°C steps from 300°C to 2000°C was used. The paints were applied on the piezo-electric gauge mounts. Exposure to the critical temperature is indicated by a glazing effect in the paint. The extent of glazing must naturally depend upon the final temperature to which the paint is raised and, therefore, to the duration of heat flux at temperatures greater than the critical; thus, accurate estimates are not obtained if the heating occurs in a pulse of short duration, as in the case of the fireball resulting from an explosion.

For obtaining data on fireball growth and movement, photographic coverage was provided. The reference fence for Fastax coverage provided scaling for all photographic coverage. For coverage other than Fastax, the rated frame speeds were used for timing. Observations were made on the horizontal diameter as the fireball grew and rose off the ground; other observations included the rate of rise and ultimate height the fireball reached.

## CALIBRATION OF INSTRUMENTATION

Primary calibration of the piezoelectric gauges was accomplished by means of a shock tube. Direct calibration of all instrumentation was accomplished by tests using known weights of high explosive, TNT.

The shock tube, FIG 5, was simply an aluminum tube, 3 feet and 5 inches long and 3 inches in diameter, with a removable driver section. Various thicknesses of aluminum foil were used to isolate the driver section, which was pressurized with dry nitrogen gas to a known pressure; the aluminum foil diaphragm then was burst by a hand-operated puncturing device. The overpressure of the resulting shock wave was calculated by an iterative solution of the following equation:

$$P_{ch} = \frac{P_s}{\left[ 1 - \left( \frac{P_s}{P_o} - 1 \right) \sqrt{\frac{7}{6 \frac{P_s}{P_o} + 1}} \right]^7}, \quad \text{Equation 1}$$

where  $P_o$ ,  $P_{ch}$ , and  $P_s$  equal atmospheric, chamber or driver, and shock absolute pressures, respectively, and the ratio of specific heats is

TABLE II  
GAUGE AND CAMERA DISTANCES FOR CLUSTER TESTS<sup>1</sup>

Piezoelectric Gauges	Self Record Gauges			Bikini Gauges			Aluminum Beam Gauges			Cameras	
	C-1	C-2	C-3	C-1	C-2	C-3	C-1	C-2	C-3	All tests	All tests
31.28	32.58	31.28	32.58	15.92	11.00	11.33	27.42	11.08	11.42	150 <sup>2</sup>	150 <sup>2</sup>
37.17	77.87	37.17	45.25	18.92	13.00	14.08	32.33	13.17	13.46	150 <sup>2</sup>	150 <sup>2</sup>
45.67	111.83	45.25	77.87	22.54	15.92	16.33	36.83	15.92	16.08	150 <sup>2</sup>	150 <sup>2</sup>
53.42				26.75	18.92	19.50	41.92	18.92	19.17	255 <sup>3</sup>	255 <sup>3</sup>
64.08				31.13	22.54	22.54	47.83	22.54	22.79	343 <sup>4</sup>	343 <sup>4</sup>
76.42				37.08	26.75	26.75	54.83	26.75	27.00	343 <sup>5</sup>	343 <sup>5</sup>
91.28				42.00	31.13	31.13	62.08	31.13	31.38		
109.25				51.25	37.08	37.08	70.75	37.08	37.33		
130.08				54.75	42.00	42.00	80.58	42.00	42.25		
156.00				46.50			88.00	46.50	46.75		
222.17											

NOTE: <sup>1</sup>All distances are in feet  
<sup>2</sup>400 fps camera  
<sup>3</sup>3000 fps camera  
<sup>4</sup>46000 fps camera  
<sup>5</sup>564 fps camera

assumed to be 1.4. Each individual gauge was calibrated with shock waves of approximately 4.3, 6.9, and 9.8 psig overpressure. The resulting gauge outputs were reduced to sensitivity coefficients in units of psi/volt (Table III). The sensitivity coefficients multiplied by the voltages obtained from a test gave the resultant overpressures.

For direct calibration tests, all instruments were set up at the selected positions, and the piezoelectric gauges were checked out by determining if finger pressure on the sensitive element registered on an oscilloscope. The outputs from the piezoelectric gauges then were connected to the tape recorder as described above.

The charges consisted of flaked TNT in 2, 5, 10, 50, and 100 pound quantities placed in cubical cardboard cartons; 1/4 pound, Nitro starch boosters and No. 8 blasting caps served as initiators. The cartons were mounted on a four foot post located at the point where the propellant tests were to be run.

A piezoelectric gauge record of a typical pressure pulse from a TNT detonation is given in FIG 6. In FIG 7, the measured overpressures for the various calibration tests are plotted versus the reduced distances, i.e., the gauge distance divided by the cube root of the charge weight and the resulting points are compared to a reference TNT overpressure-reduced distance curve which was developed as a part of this study. The data points generally followed the reference curve with the largest percentage deviations corresponding to the lowest pressures, this, probably, being partly caused by failure to apply corrections for wind velocity and ambient temperature.

The piezoelectric gauges also were used for determining shock wave velocity since they indicated the time of arrival of the shock wave at given locations. By curve fitting the time of arrival data and differentiating the resulting polynomials, point estimates were obtained of shock wave velocity as a function of distance from each calibration test. These estimates were used for calculating the corresponding overpressures by means of the following equation:

$$P_P = P_0 \left( \frac{2\gamma}{\gamma + 1} \right) \left( \frac{U^2}{C^2} - 1 \right), \quad \text{Equation 2}$$

where  $P_P$  is the peak shock overpressure,  $P_0$  is the atmospheric pressure,  $\gamma$  is the ratio of specific heats,  $C$  is the velocity of sound, and  $U$  is the shock wave velocity. Because no zero time signal was used, times of arrival at various locations were measured relative to the time of arrival of the shock wave at the closest gauge position. Overpressures obtained by this method generally were similar to overpressures measured directly and, therefore, are not included.

For the backup instrumentation, calibration was determined with the TNT tests. The foilmeter readings were converted to overpressures by means of the published calibration curves and plotted against the



TABLE III  
SENSITIVITY COEFFICIENTS FOR PIEZOELECTRIC GAUGES

TEST NO. C-1			TEST NO. C-2			TEST NO. C-3		
Gauge Number	Sensitivity Coefficient, psi/v	Gauge Number	Sensitivity Coefficient, psi/v	Gauge Number	Sensitivity Coefficient, psi/v	Gauge Number	Sensitivity Coefficient, psi/v	Gauge Number
1	23.00	1	23.00	1	23.00	1	9.66	
2	-	2	-	2	-	2	-	
3	4.01	3	4.01	3	4.01	3	4.01	
4	34.75	4	34.75	4	34.75	4	34.75	
5	16.05	5	16.05	5	16.05	5	16.05	
6	4.41	6	4.41	6	4.41	6	4.41	
7	12.77	7	12.77	7	12.77	7	12.77	
8	10.11	8	10.11	8	10.11	8	10.11	
9	5.47	9	5.47	9	5.47	9	5.47	
10	8.69	10	8.69	10	8.69	10	8.69	
11	-	11	-	11	-	11	-	
12	18.78	12	18.78	12	18.78	12	18.78	

reduced distances for the various calibration tests. The results, shown in FIG 8, were distributed about the reference TNT curve, the agreement being surprisingly good in view of the all-or-none character of the burst diaphragm measurements.

Although the cantilever beam results for the calibration tests were entirely consistent with the published calibration curves, the results for the propellant tests (discussed below) exhibited certain peculiarities not previously reported and which are difficult to discuss in terms of the corresponding overpressures. For this reason, the results are presented in FIG 9 in the form of permanent tip deflections versus distances from a given TNT explosion. Inspection of the plotted data indicates satisfactory agreement with the published reference curves,

No published calibration curves were available for the self record gauges. Therefore, the data for the calibration tests were used to establish the deflection versus reduced distance plot shown in FIG 10. Inasmuch as the piezoelectric gauge data previously had confirmed the applicability of the standard TNT curve to these tests, the deflection for any given reduced distance could be converted readily to the corresponding overpressure by means of the standard TNT curve.

From the Fastax coverage, the velocity of the shock wave could be determined by measuring the slope of the distance-time curve for the shock wave. During calibration tests, timing marks were not recorded on the Fastax film, and precise calibration data, therefore, were not obtained. However, FIG 11 is a plot of results for a 50 pound test using the number of frames in lieu of timing marks. Timing marks were recorded on the film for the propellant tests. Overpressures were calculated from the Fastax time-of-arrival data in the manner described earlier for the piezoelectric gauge time-of-arrival data. However, it should be noted that shock waves visible on Fastax film are limited to those for which the overpressures are greater than approximately 2 to 3 psi. In this study, visible shocks were noted for calibration tests using as little as 10 pounds of TNT.

## RESULTS

### Fragmentation

The fragmentation patterns for the Single Tank Tests, S-1 and S-2, are shown in FIG 12 and 13. Although the number of fragments was small for each test, the larger number of fragments and the wider range of dispersion noted for test S-1 may have been due to embrittlement of the tank material by the low temperature of the LOX. Evidence of this also was afforded by the irregular edges of the fragments.

The fuel container for test S-2 remained substantially intact except for the ends. Both tanks showed the clean cutting action of the FLSC at the line of contact. Some evidence of partial splitting was noticed

along the weld seam of both tanks. Aside from the wall splitting, both hemispherical ends of each tank were blown off. Failure occurred at the weld seams.

Inasmuch as the purpose of the single tank tests was to qualify the external destruct system, no blast instrumentation was provided. As expected, visual and photographic monitoring of the test failed to indicate any explosions associated with the propellants although the RP-1 was ignited by the destruct action and burned for several hours.

The fragmentation patterns for the cluster tests, C-1, C-2, and C-3, are shown in FIG 14, 15, and 16. The three fragments found after the first test using an external destruct system, C-1, were parts of the upper fuel venting line to which the Primacord ringline was attached. The fuel container which fell ten feet away was the only part of the clusters blown away due to either exploding of the propellants or splitting of the tanks. This particular container was adjacent to the FLSC strip on the inner LOX tank. The results indicated that the destruct system functioned satisfactorily and that the dispersion of the propellants was complete except for a small quantity of RP-1 which remained in the lower hemispherical bulkheads.

In an attempt to disperse the small amount of RP-1 remaining in the bulkheads, the external destruct system for test C-2 was modified as indicated previously. For this test, all of the tanks remained on the test stand after destruct action. The fragments consisted of pieces of the fuel venting line except for a skirt from the bottom of one fuel tank which was detached from the tank by the FLSC and not by a propellant explosion. This piece was observed in the motion pictures to roll and tumble along the ground. All of the propellants were dispersed for this test.

For test C-3, the Primacord inside the wells of the container did not produce sufficient explosive force to disperse all of the propellants. Thus, the walls of most of the containers were only partially ruptured, and a large quantity of RP-1 was left in the containers after the test. One fuel container was ruptured only at the upper bulkhead. The center LOX container and one RP-1 container were substantially undamaged. One outer LOX container received only minor damage because the Primacord did not propagate due to improper attachment to the ringline.

Despite the fact that the Primacord used was insufficient to effect complete dispersion of all the propellants, severe fragmentation resulted for those containers whose contents were dispersed, and all of the containers were blown off the test stand. Presumably, if Primacord of sufficient explosive force to effect complete dispersion had been used, fragmentation of the containers would have been even more extensive.

Because the explosive force and fireball resulting from test C-3 cannot be attributed to that portion of the propellants which was not

actually dispersed, data obtained from this test were calculated on the basis of an assumed total propellant weight of 1700 pounds, or roughly 50 percent of the actual total. The explosive yield from the test was so low that differences of even several hundred pounds in the assumed total propellant weight were not critical; consequently, no attempt was made to obtain a better estimate.

### Fireball

Fireball observations and measurements were based almost entirely on photographic records. After activation of the destruct system for each of the cluster tests, ignition apparently took place immediately; no delay was detected even by inspection of individual frames of the Fastax films. This suggests that any delay must have been of the order of 150 micro-seconds or less.

The sizes of the fireballs as a function of time after ignition are shown in FIG 17. For test C-1, the ground level fireball diameter increased at a steadily decreasing rate for approximately 2 seconds, at which time it lifted off the ground. The maximum diameter was approximately 100 feet and occurred after about 2.5 seconds; the visible flame was extinguished after about 4 seconds. The fireball for test C-2 increased in size at a steadily decreasing rate until the visible flame was extinguished after about 2.5 seconds, at which time the diameter was approximately 140 feet.

For test C-3, the fireball was appreciably smaller, the maximum diameter being about 90 feet. This was undoubtedly due, in part, to the smaller quantity of propellants dispersed.

In addition to the ground level fireball, a mushroom type fireball appeared in each test about 2 seconds after ignition and grew to approximately the same size as the ground level fireball by the time the visible flame was extinguished. At that time, the top of the mushroom type fireball had reached an altitude of approximately 150 feet.

Visual observation at the time of the tests showed apparent horizontal symmetry in the fireballs of tests C-1 and C-2, but helicopter motion pictures and the soot markings on the ground surrounding the tanks indicated that star-shaped dispersion patterns developed initially and quickly degenerated into spherical patterns. Fastax camera records from the ground tended to confirm this finding. The fireball for test C-3 was irregularly shaped, both on the ground and in the air.

Estimates of temperatures in the vicinity of the fireballs were obtained by use of "Tempilaq" paints and were relatively crude. These paints were placed on the piezoelectric gauge mounts. High speed photography showed that after ignition the first few mounts were enveloped by the expanding oxygen vapors and then were exposed to the fireball. It could not be determined if the fireball actually touched the mounts, so it is not known whether the temperatures were due to

radiant heating or actual flame contact. However, some very light sooting was noted on the first two mounts although the maximum indicated temperatures were relatively low. Table IV indicates the approximate temperatures at various distances from the center of the charges.

Probably, the maximum temperatures for tests C-1 and C-2 were appreciably higher than the values shown due to the relatively short duration of the exposures. Test C-3 gave no distinct estimate. This suggests that the temperatures were much lower than for the other tests and is consistent with the smaller fireball diameter and the smaller quantity of propellants dispersed.

TABLE IV

Approximate Temperature Profiles

Distance from Ground Zero	Test		
	C-1	C-2	C-3
31 feet	500°C	500°C	-
37 feet	500°C	500°C	-
45 feet	300°C	300°C	-
53 feet	300°C	300°C	-

Shock Waves

Overpressures for the cluster tests were obtained directly from the amplitudes of the peaks obtained with the piezoelectric gauges and indirectly from the times between corresponding peaks for different piezoelectric gauges. Indirect estimates of overpressure also were obtained from the self record gauges by relating the measured deflections for any given value of Z in the calibration tests to equivalent overpressures for corresponding values of reduced distance.

None of the foilmeter diaphragms were ruptured during the cluster tests although several were melted by the heat. Similarly, inspection of the Fastax films failed to indicate visible shock waves. Comparison of these results with those for the calibration tests indicated that the yields for the cluster test must have been on the order of ten pounds of TNT or less.

The cantilever beam results shown in FIG 18 confirm the very low yields indicated by the foilmeter and Fastax results. However, it is of interest to note that some of the gauges indicated negative tip deflections, whereas previous investigators have reported only positive

deflections. The physical significance of this phenomenon is not immediately evident but may be related to the large heat flux resulting from the propellant explosions. This possibility is supported by the fact that a few of the closest gauges were melted by the intense heat.

Whereas the foilmeter and cantilever beam gauges are capable of only a single indication for each test, the self record and piezoelectric gauge systems provided continuous monitoring capable of differentiating between explosions occurring only a few milliseconds apart. Inspection of the results indicated that multiple explosions occurred during each cluster test (See Table V). Moreover, inspection of the individual pressure time trace indicated that in no instance was the first explosion the largest.

Self record and piezoelectric gauge results for the largest explosion for each of the three cluster tests are summarized in FIG 19, 20, and 21. Also included in these figures are curves corresponding to yields of 100, 10, 1, and 0.1 percent TNT calculated from the reference curve shown in FIG 6. The piezoelectric gauge system failed to function for test C-1. However, the overpressure data for the self record gauges indicated a yield of approximately 0.05 percent or 1.7 pounds of TNT. For test C-2, overpressures were obtained for both the self record and piezoelectric gauges and indicated a yield of approximately 0.1 percent or 3.5 pounds of TNT. For test C-3, overpressures were obtained for both types of gauges and indicated a yield of approximately 0.3 percent or 5 pounds of TNT. Overpressures calculated indirectly from the piezoelectric gauge time of arrival data were in general agreement with the directly measured overpressures and are not given.

TABLE V

Number of Significant Explosions Indicated by  
Different Types of Instrumentation

	<u>Test C-1</u>	<u>Test C-2</u>	<u>Test C-3</u>
Visible (Film Examination)	3	6	6
Self Record Gauges	4	7	6
Piezoelectric Gauges	-	1	6

CONCLUSIONS

A comparison of the low yields (<0.5 percent) obtained in this study with those determined in previous destruct tests failed to confirm the expected increase in yield due to the cluster configuration of the Saturn I booster. This suggests that, as long as the ignition

delay time after release of the propellants is essentially nil, even major increases in interface area do not result in high yields.

Comparisons of the results for the different destruct systems indicated significantly lower yields for the external FLSC system. However, all yields were close to the lower limit which could be measured with the available instrumentation. Therefore, it is difficult to estimate quantitative differences to be expected in full scale tests of these systems.

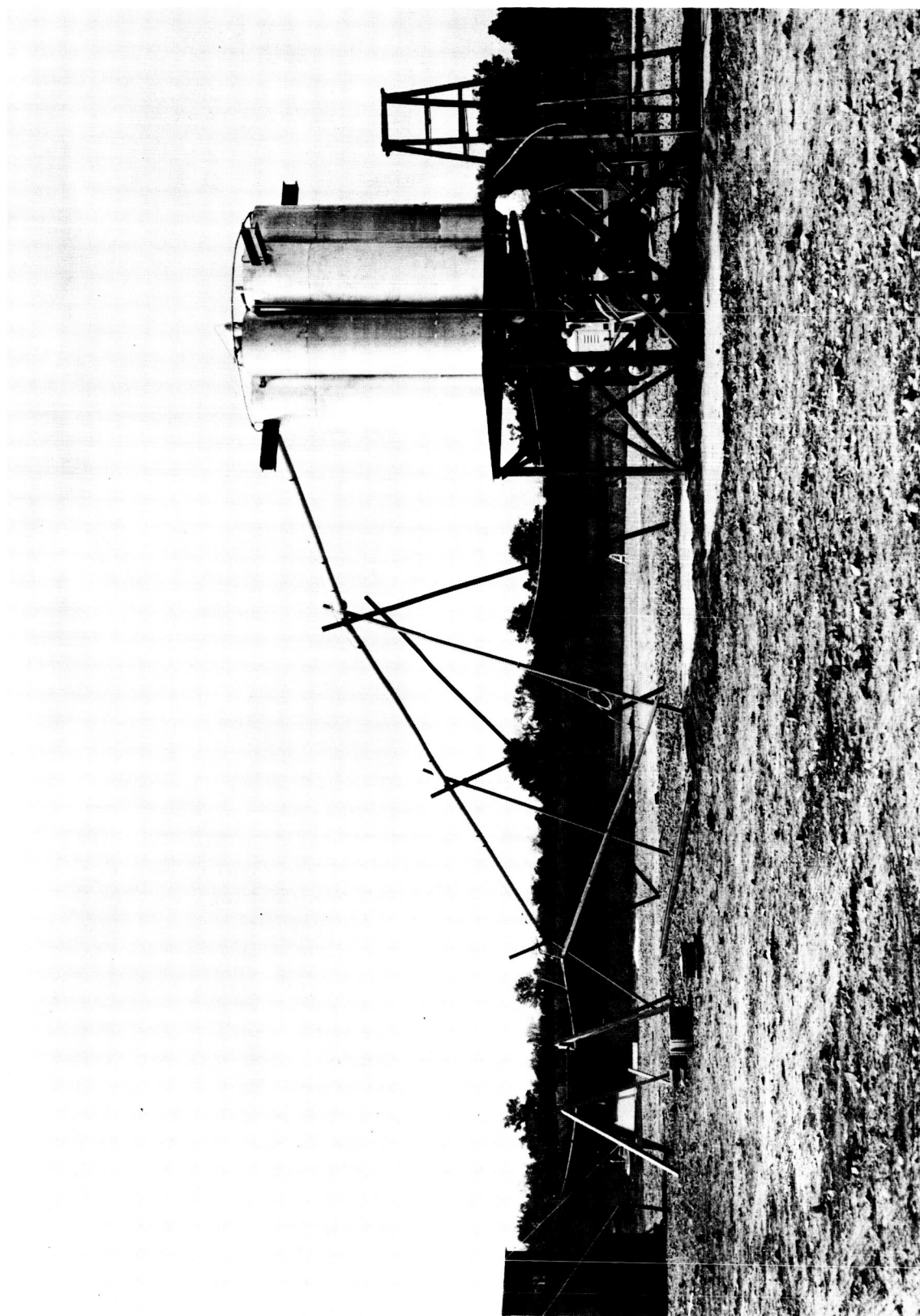
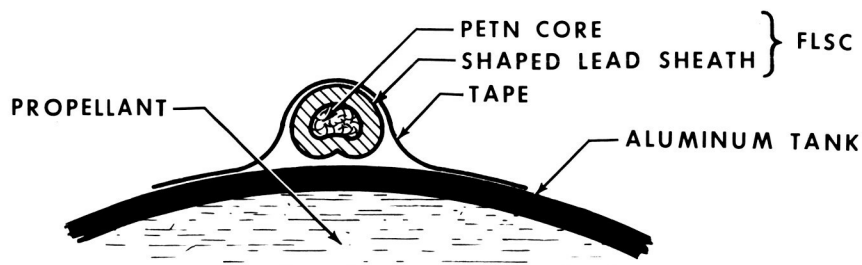
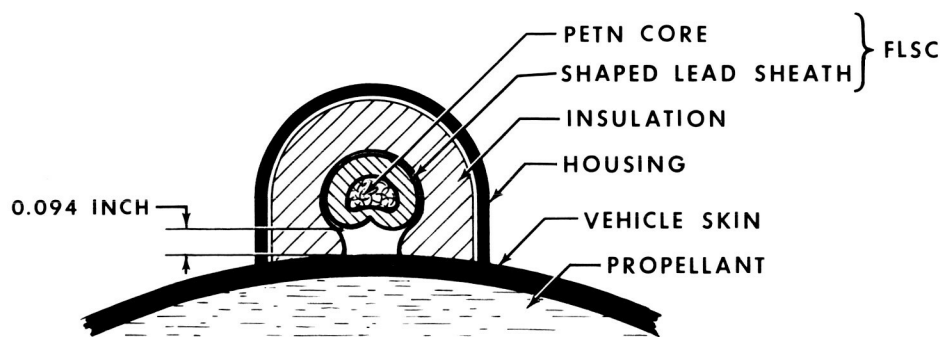


FIGURE 1. CLUSTER IN PLACE AT TEST SITE

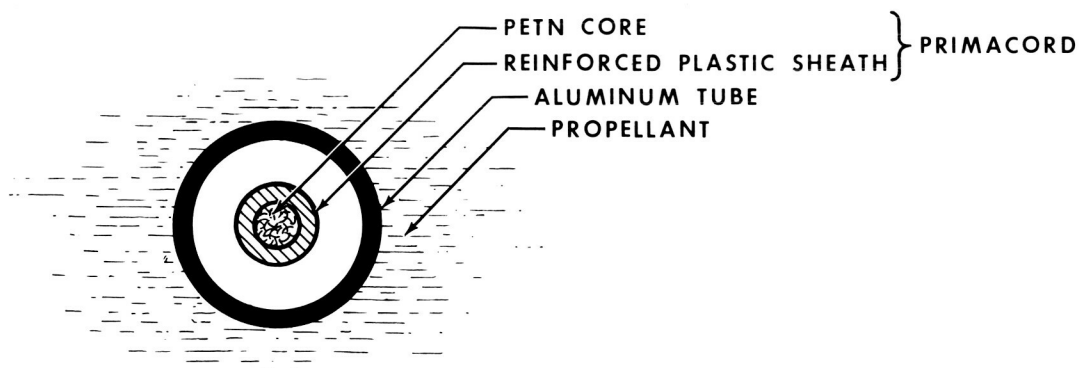




a. EXTERNAL DESTRUCT SYSTEM (TEST CONFIGURATION)



b. EXTERNAL DESTRUCT SYSTEM (FLIGHT CONFIGURATION)



c. INTERNAL DESTRUCT SYSTEM

FIGURE 2 DETAILS OF DESTRUCT SYSTEMS

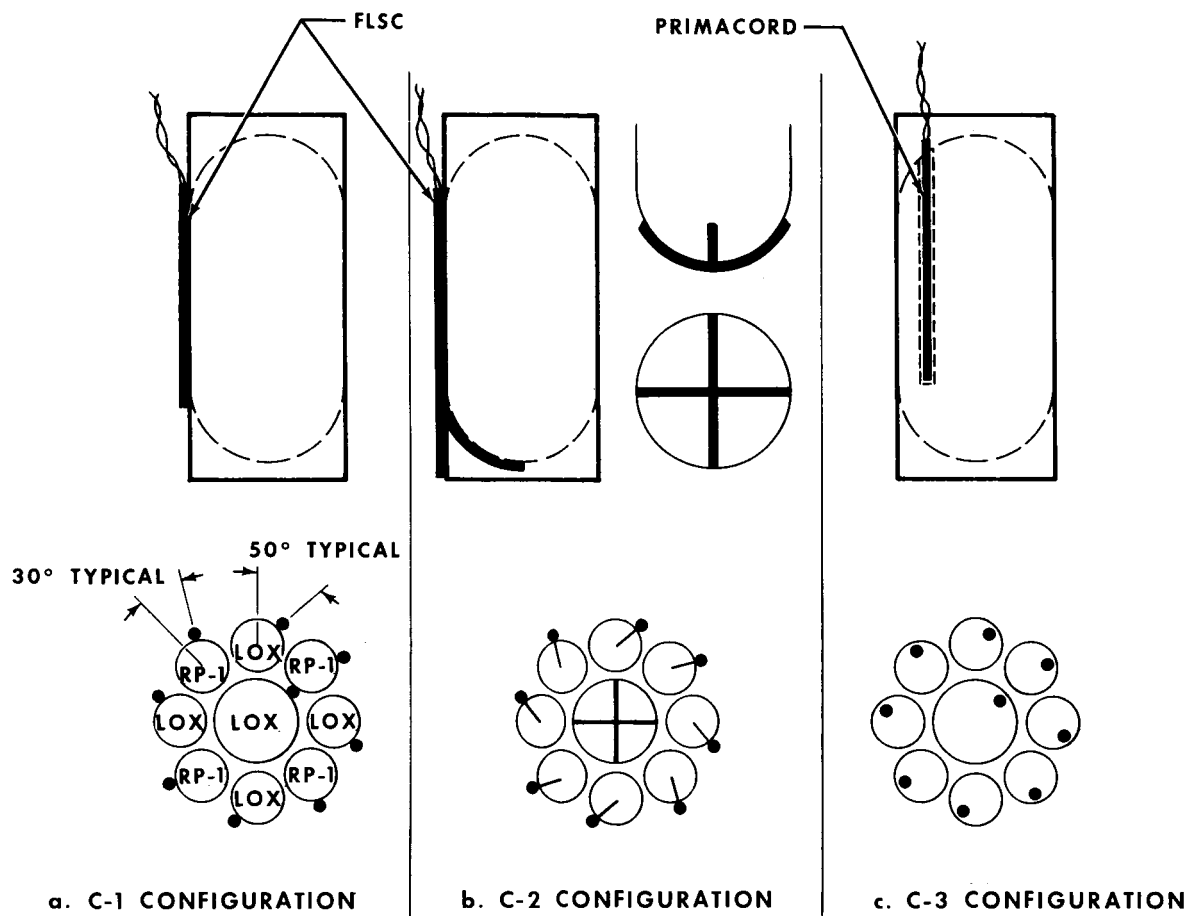


**FIGURE 3 LOCATION OF DESTRUCT SYSTEMS**

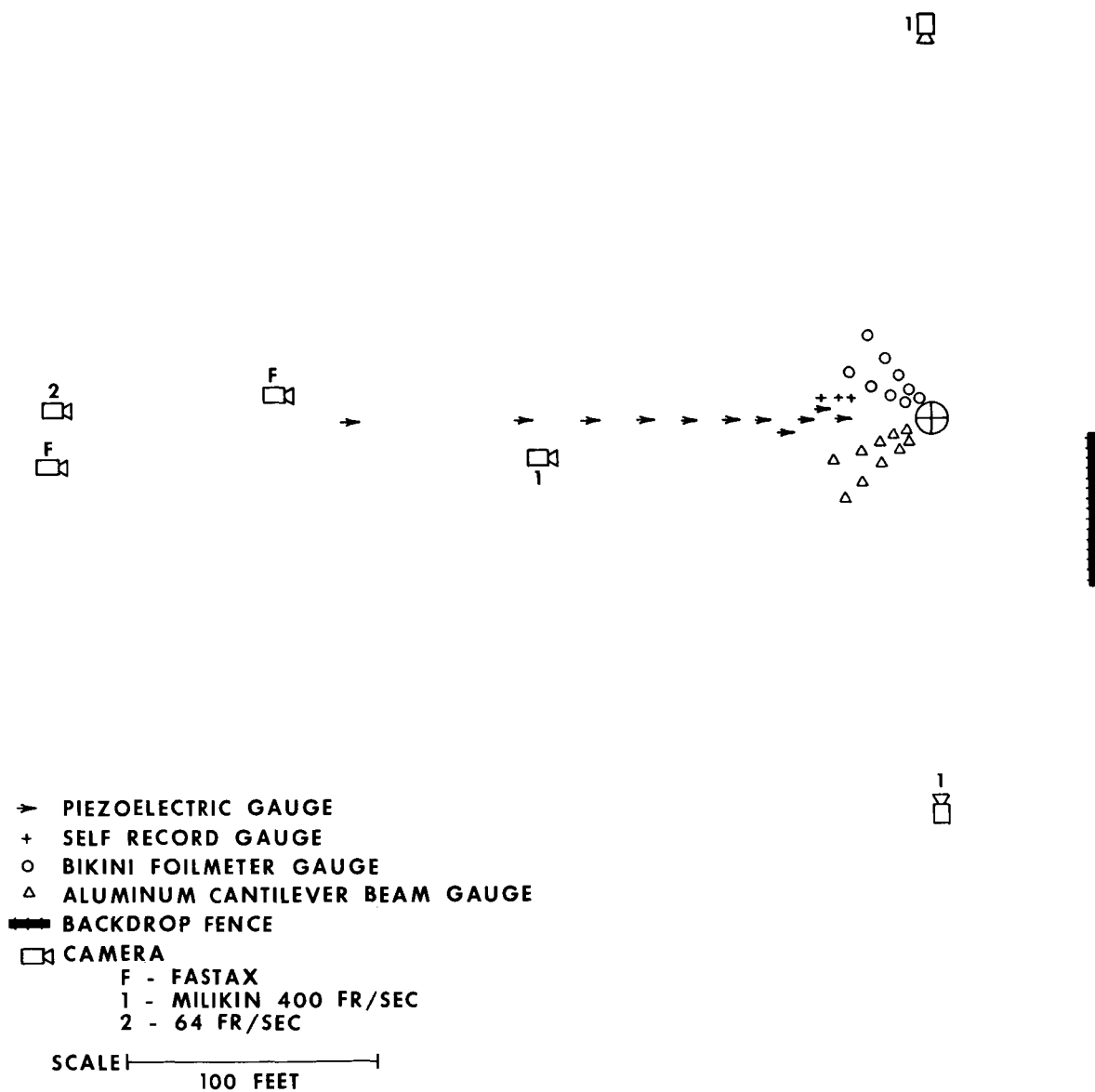
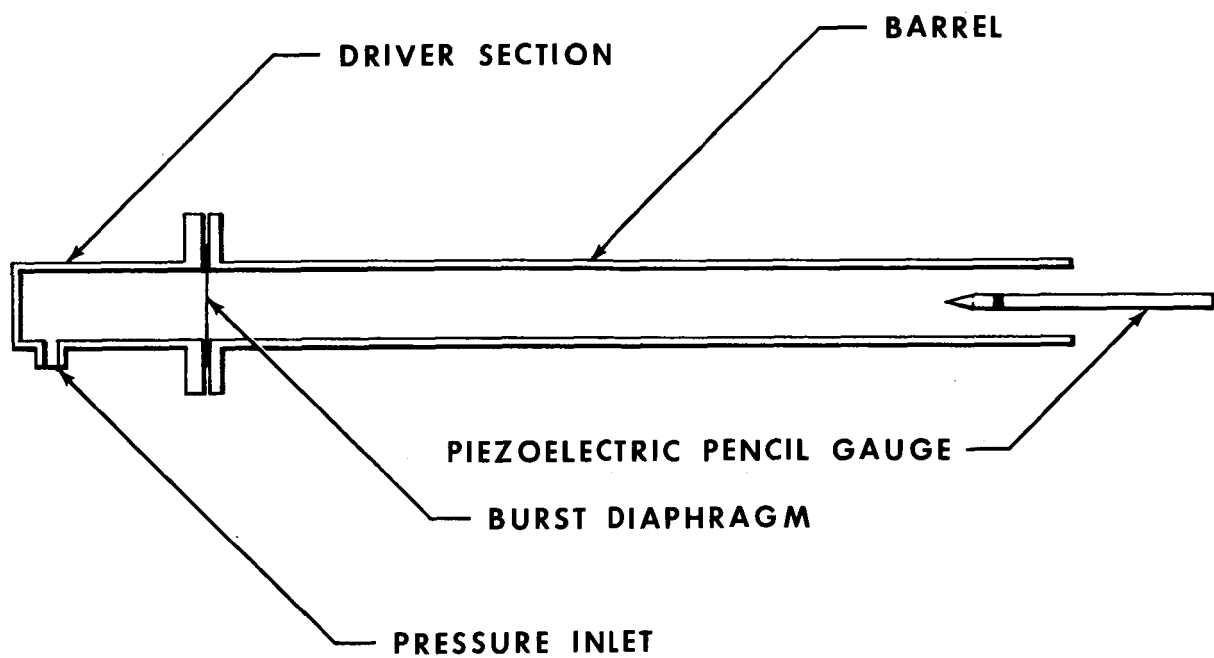
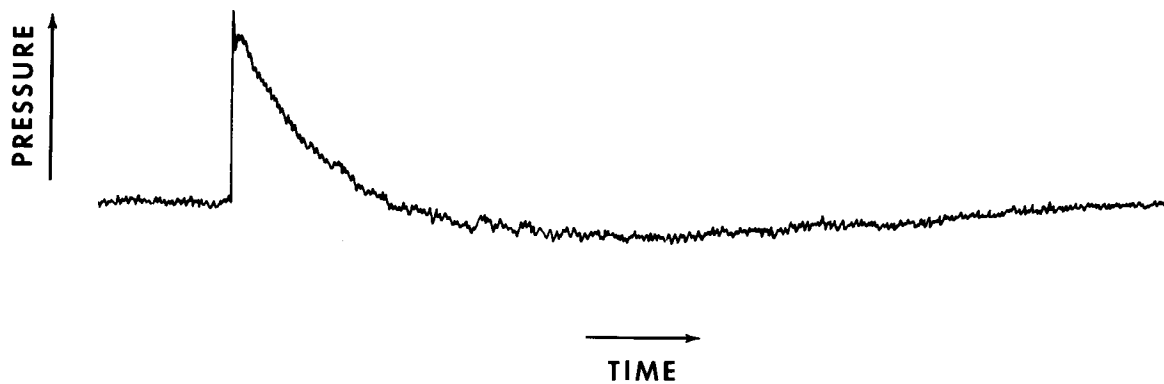


FIGURE 4 BLAST INSTRUMENTATION LAYOUT



**FIGURE 5 SHOCK TUBE USED FOR CALIBRATION**



**FIGURE 6 OSCILLOSCOPE TRACE FOR  
TYPICAL SHOCK WAVE**

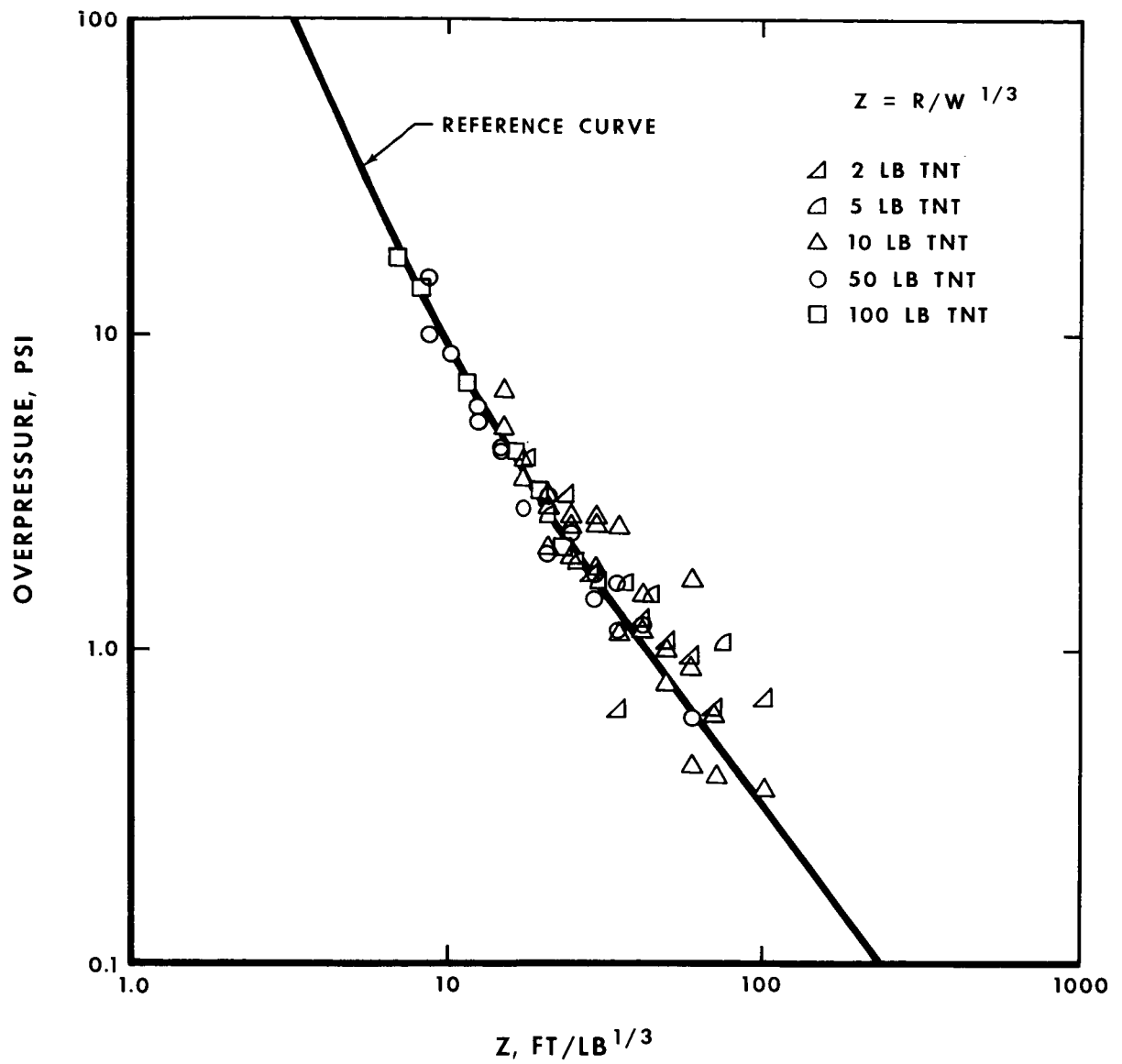


FIGURE 7 CALIBRATION DATA AND REFERENCE CURVE FOR PIEZOELECTRIC GAUGES

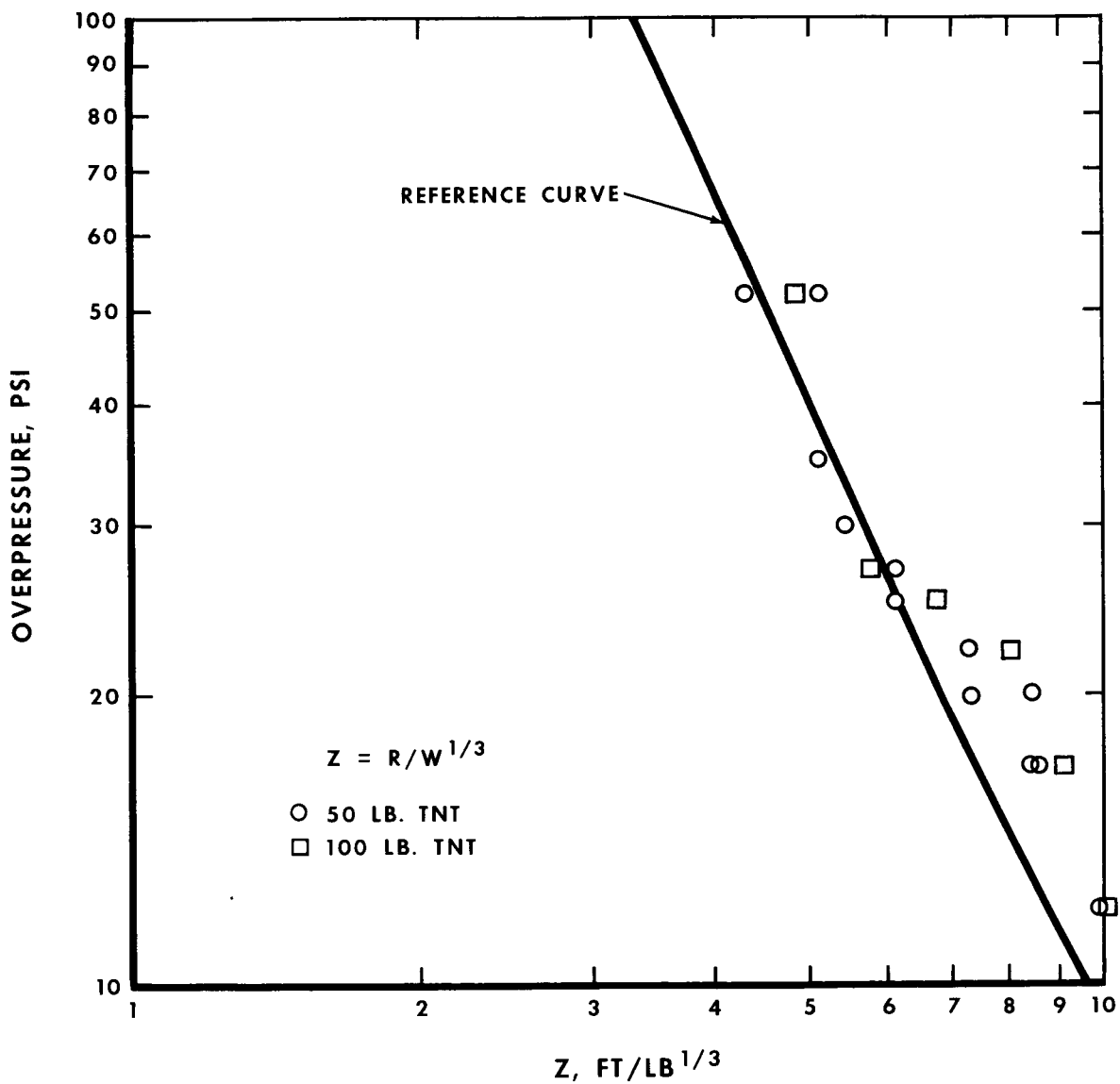


FIGURE 8 CALIBRATION DATA AND REFERENCE CURVE FOR FOILMETER GAUGES

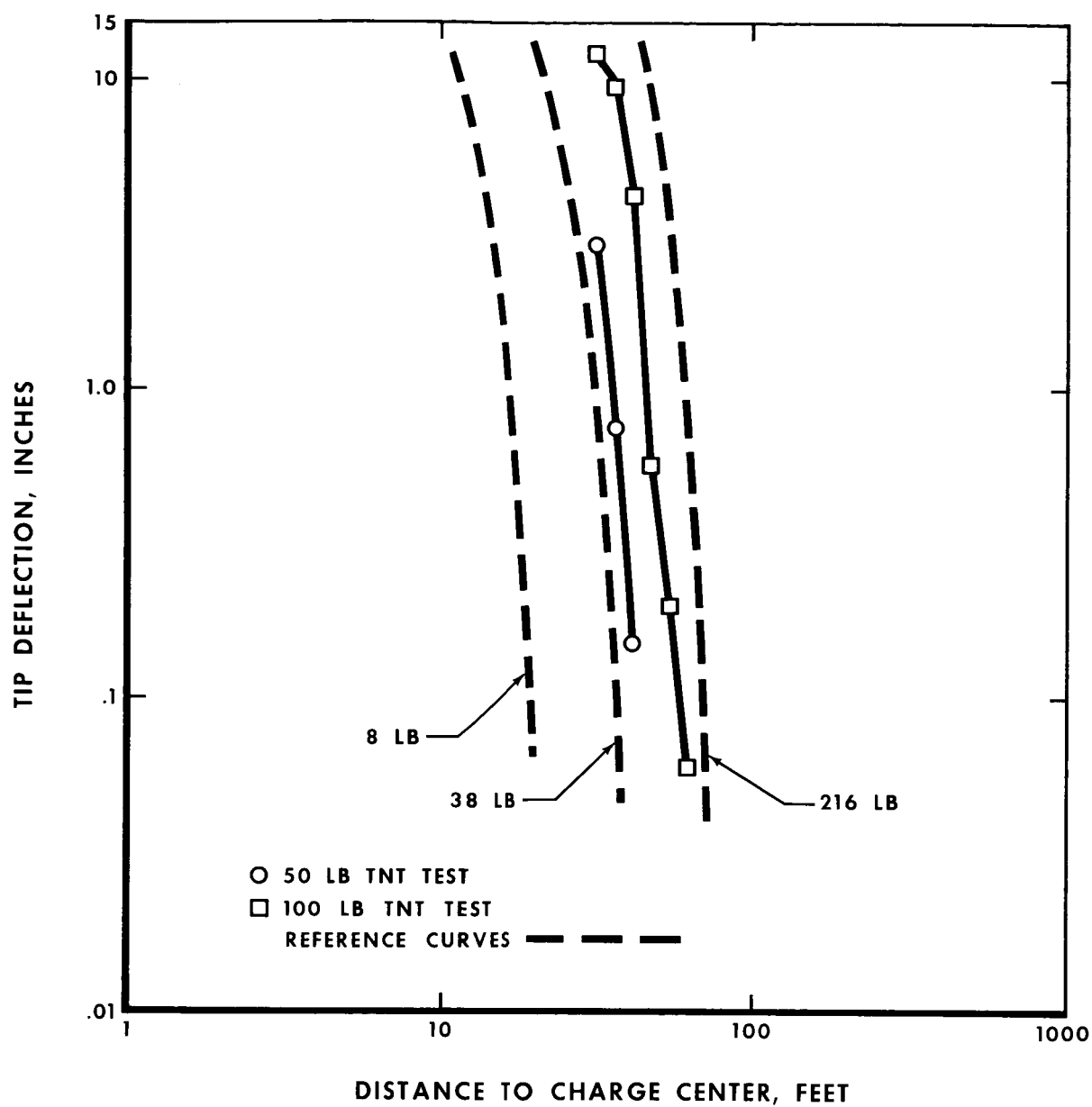


FIGURE 9 CALIBRATION DATA AND REFERENCE CURVES FOR CANTILEVER BEAM GAUGES.



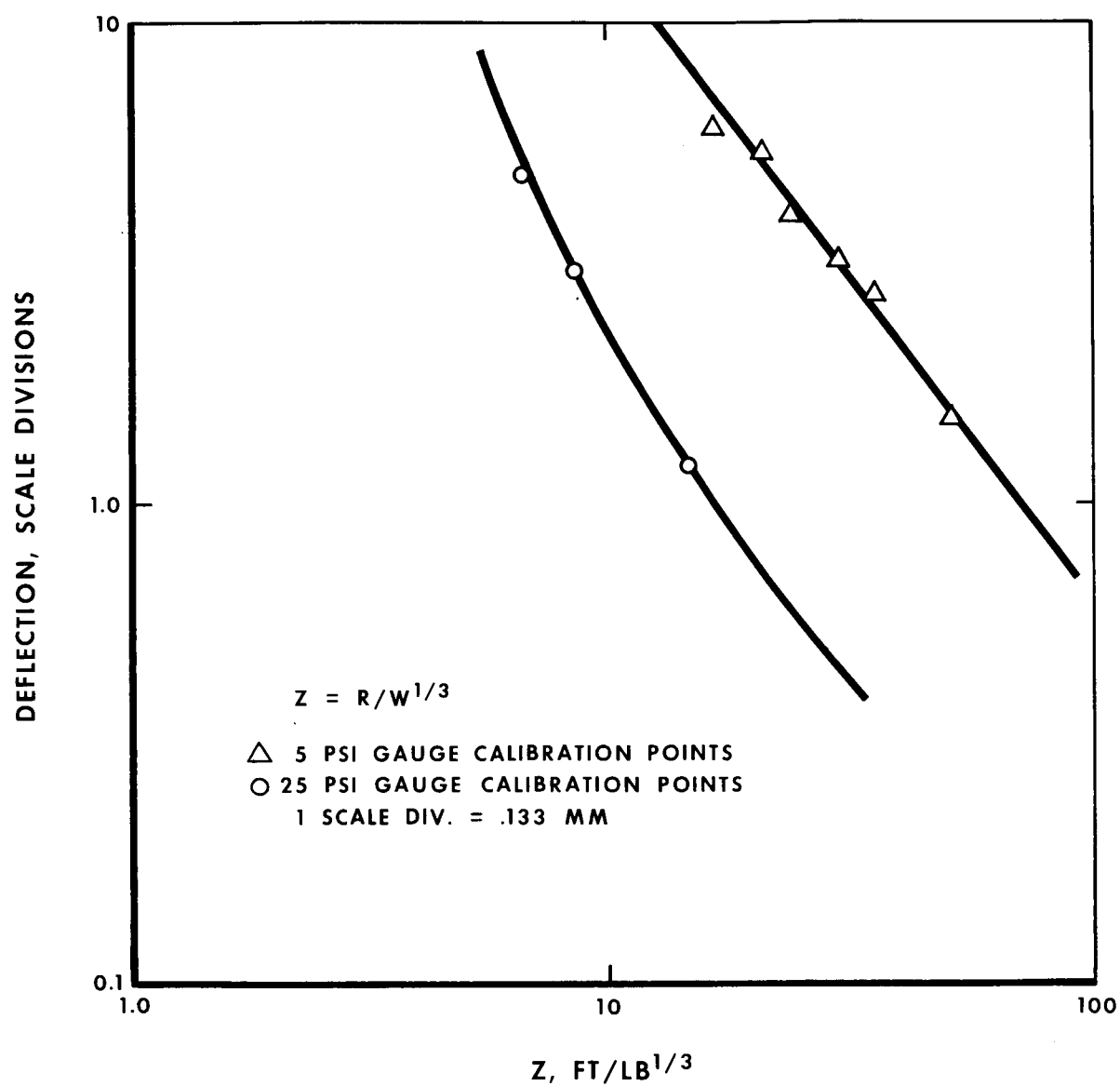
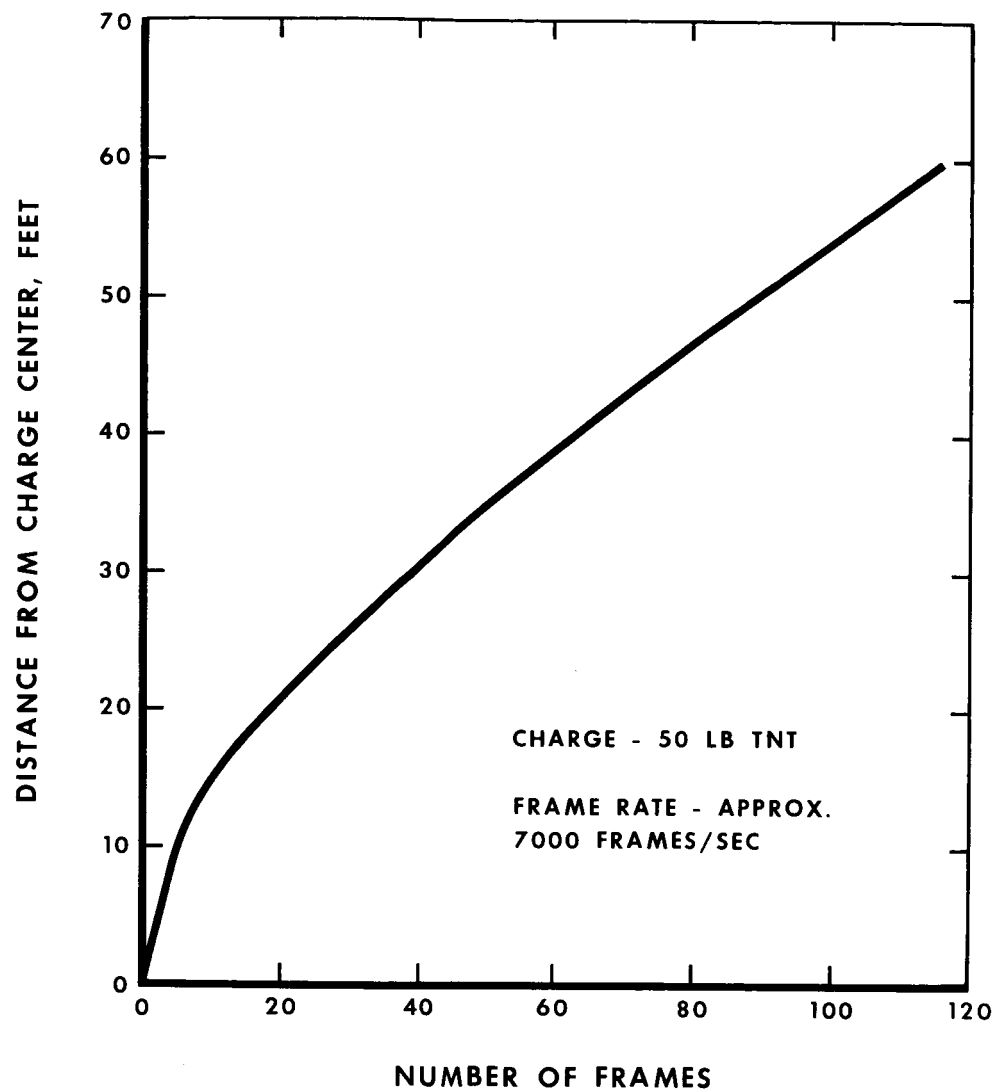
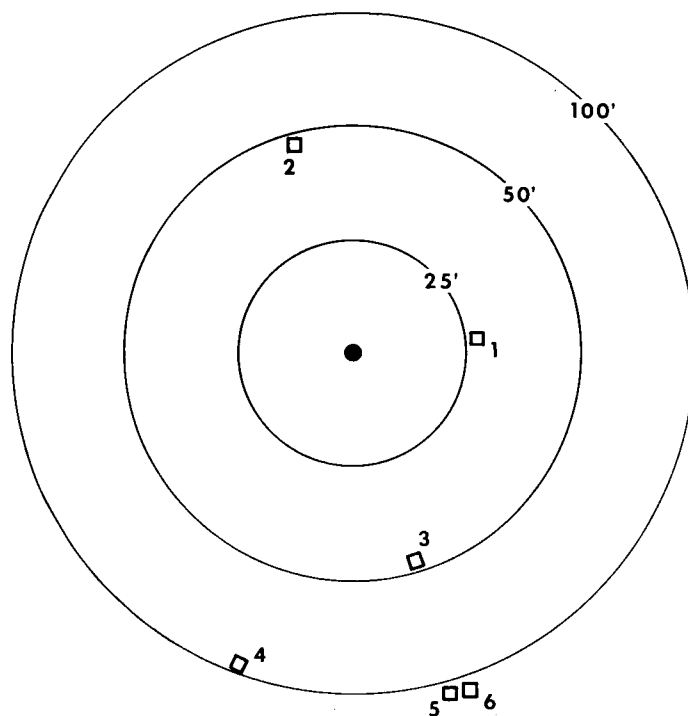


FIGURE 10 CALIBRATION DATA FOR SELF - RECORD GAUGES



**FIGURE 11 TIME OF ARRIVAL OF SHOCK WAVE  
AS MEASURED WITH FASTAX CAMERA**

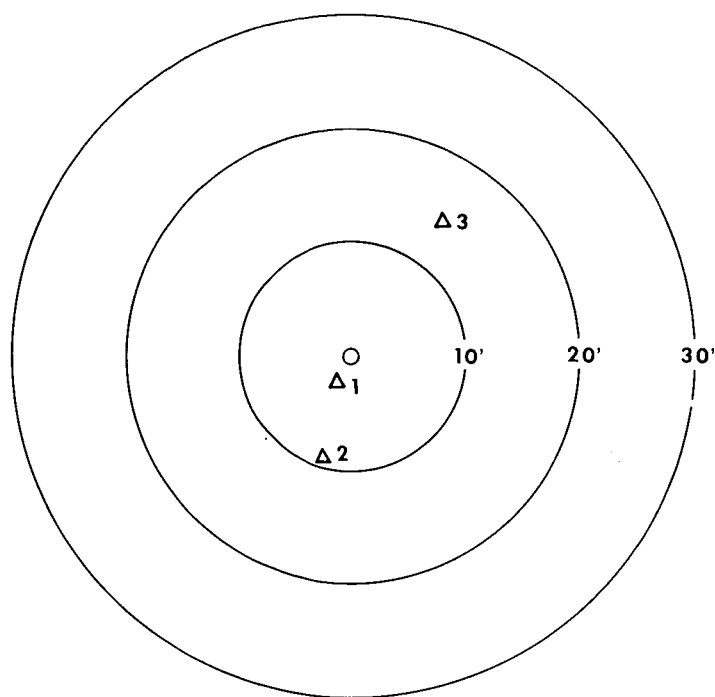


FRAGMENT NO.	DISTANCE FROM CHARGE CENTER, FT	WEIGHT	
		LBS	OZS
1	27	3	8
2	46	4	0
3	48	16	0
4	90	4	0
5	105	5	0
6	106	3	0

● LOX CONTAINER

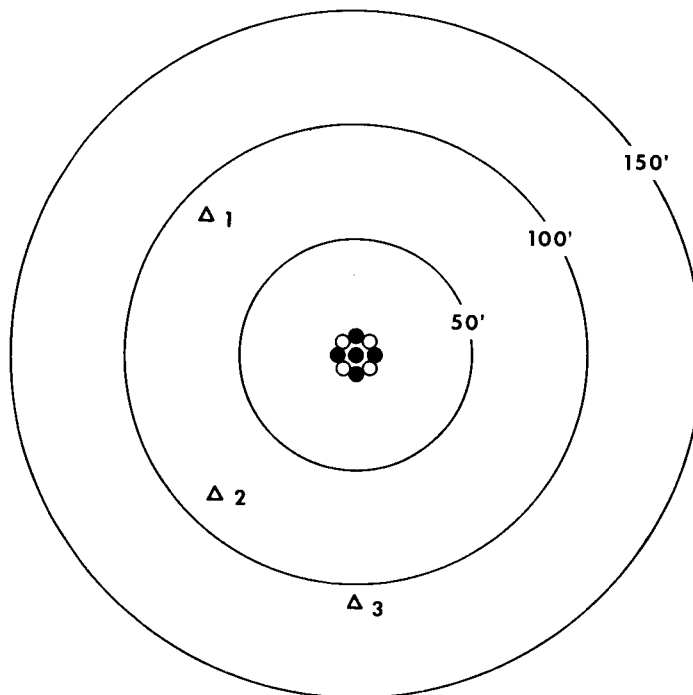
□ LOX CONTAINER  
FRAGMENTS

FIGURE 12 FRAGMENT PATTERN FOR SINGLE LOX CONTAINER,  
TEST S-1



FRAGMENT NO.	DISTANCE FROM CHARGE CENTER, FT	WEIGHT		○ RP-1 CONTAINER △ RP-1 CONTAINER FRAGMENTS
		LBS	OZS	
1	3	12	8	
2	9	38	0	
3	13	6	0	
4	33	3	5	

FIGURE 13 FRAGMENT PATTERN FOR SINGLE FUEL CONTAINER,  
TEST S-2



FRAGMENT NO.	DISTANCE FROM CHARGE CENTER, FT	WEIGHT	
		LBS	OZS
1	90	0	2
2	82	0	3
3	105	0	2

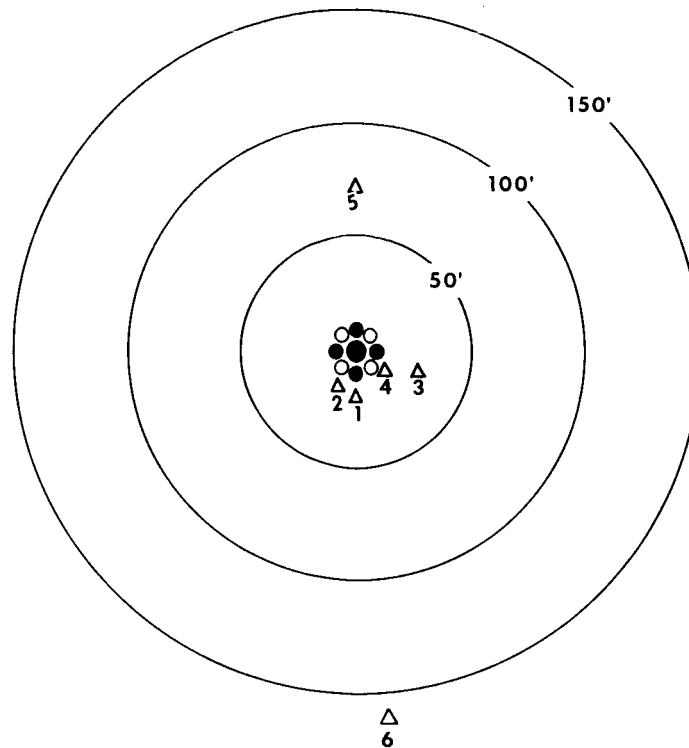
● LOX CONTAINER

○ RP-1 CONTAINER

□ LOX CONTAINER FRAGMENTS

△ RP-1 CONTAINER FRAGMENTS

**FIGURE 14 FRAGMENT PATTERN FOR TEST C-1  
(EXTERNAL DESTRUCT SYSTEM)**



FRAGMENT NO.	DISTANCE FROM CHARGE CENTER, FT	WEIGHT		
		LBS	OZS	
1	14	0	3	● LOX CONTAINER
2	11	0	8	○ RP-1 CONTAINER
3	28	0	3	□ LOX CONTAINER FRAGMENTS
4	16	0	2	△ RP-1 CONTAINER FRAGMENTS
5	71	0	12	
6	165	1	2	

**FIGURE 15 FRAGMENT PATTERN FOR TEST C-2  
(EXTERNAL DESTRUCT SYSTEM)**

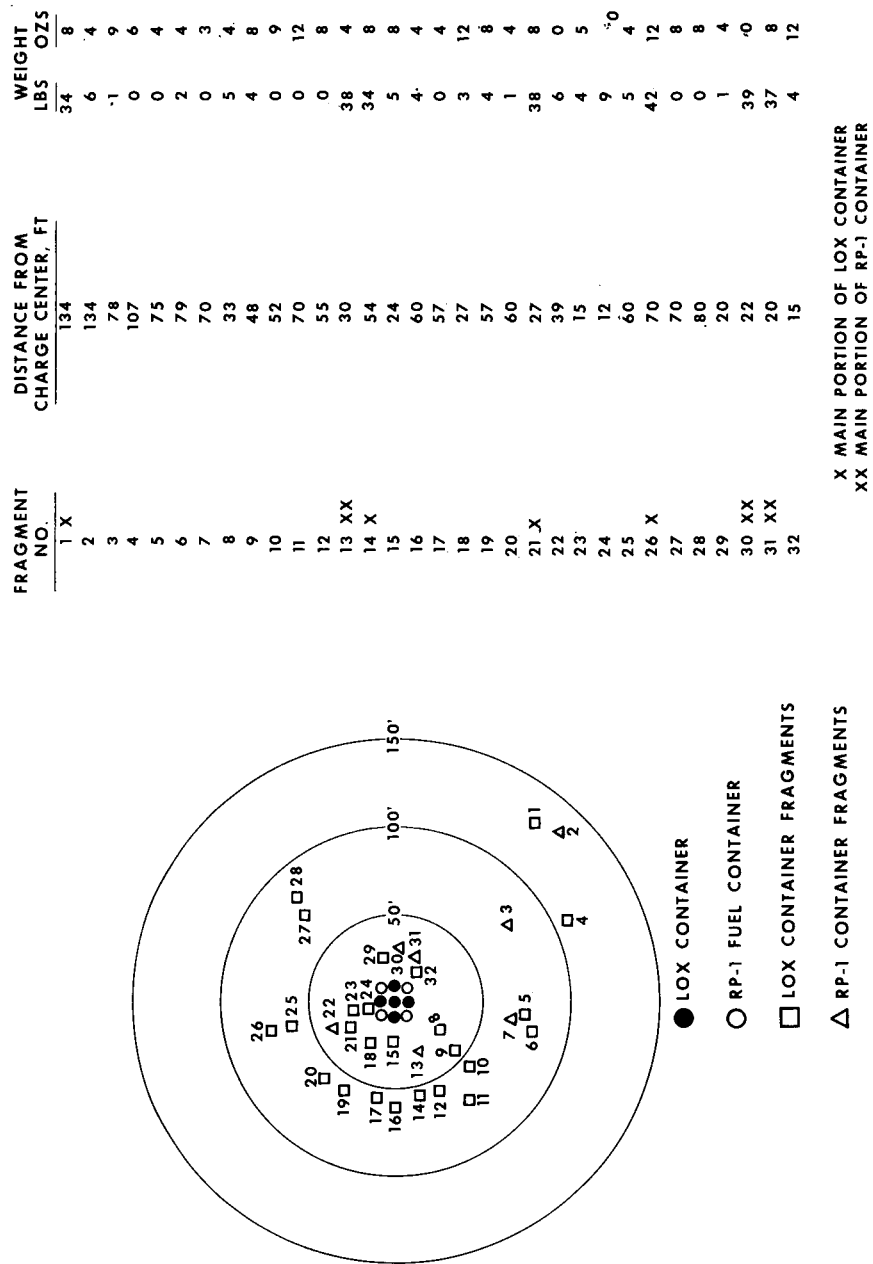


FIGURE 16 FRAGMENT PATTERN FOR TEST C-3 (INTERNAL DESTRUCT SYSTEM)

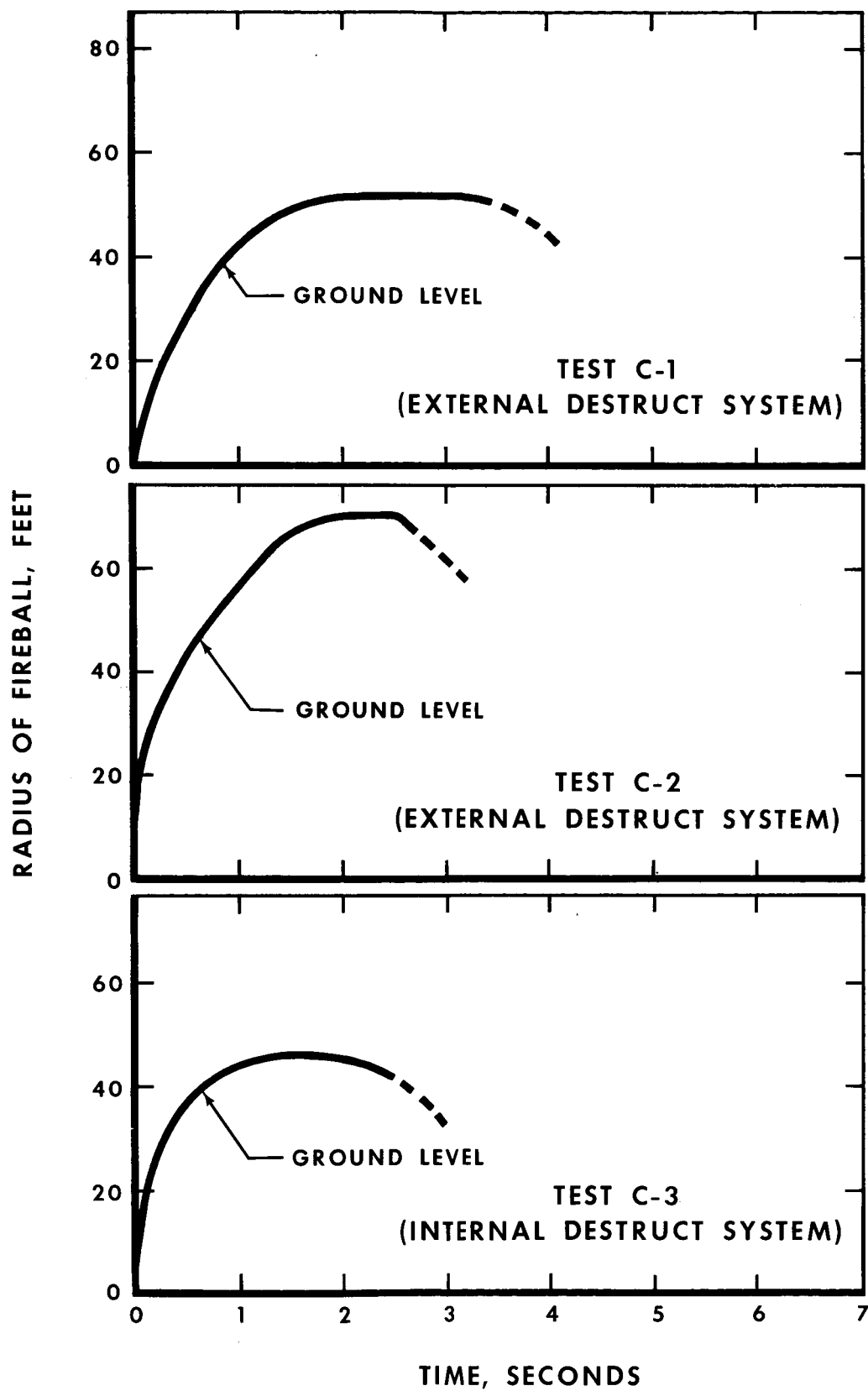


FIGURE 17 FIREBALL SIZE AND DURATION FOR CLUSTER TESTS



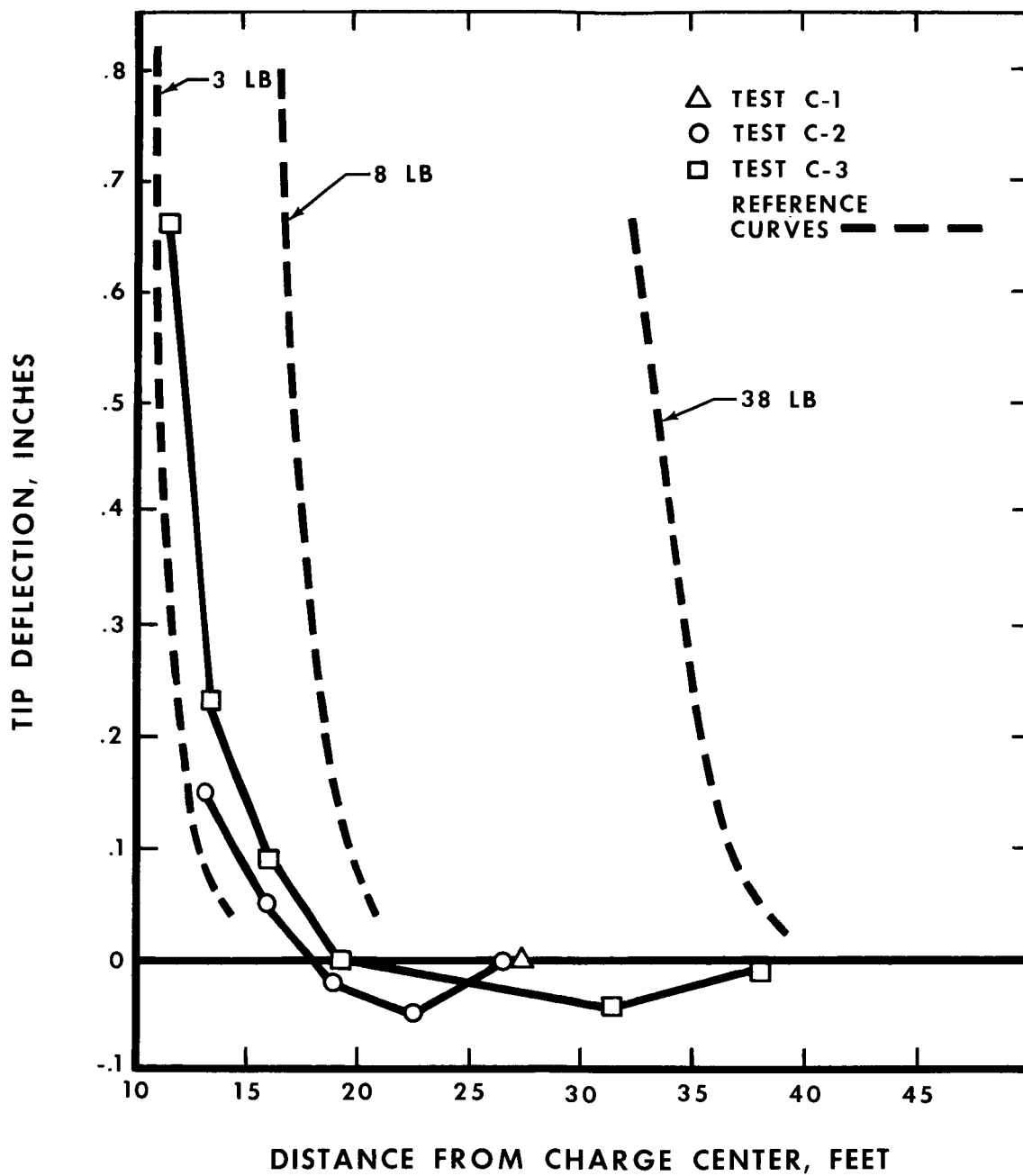


FIGURE 18 CANTILEVER BEAM DATA FOR CLUSTER TESTS

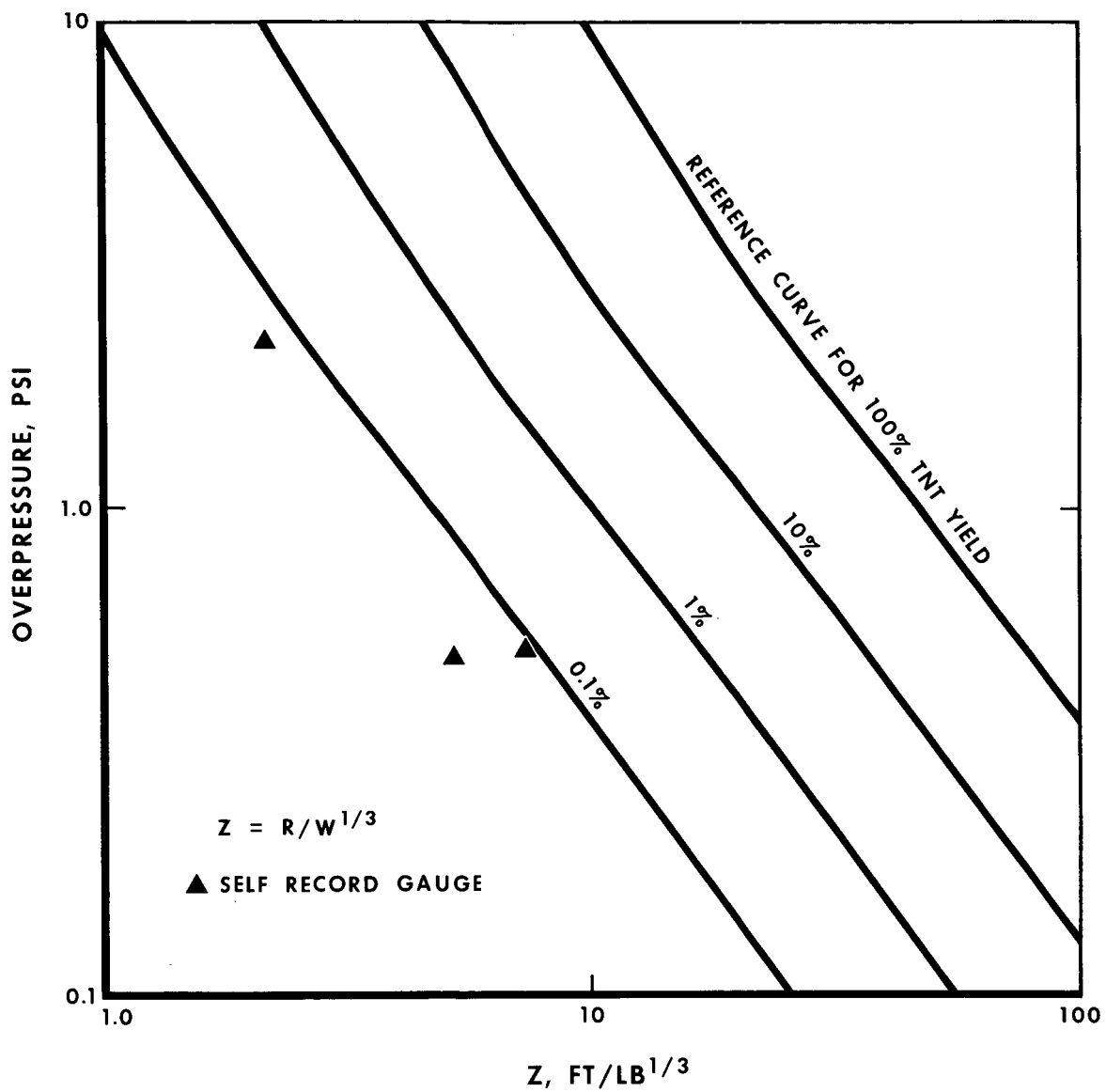


FIGURE 19 EQUIVALENT TNT YIELD FOR TEST C-1  
(EXTERNAL DESTRUCT SYSTEM)

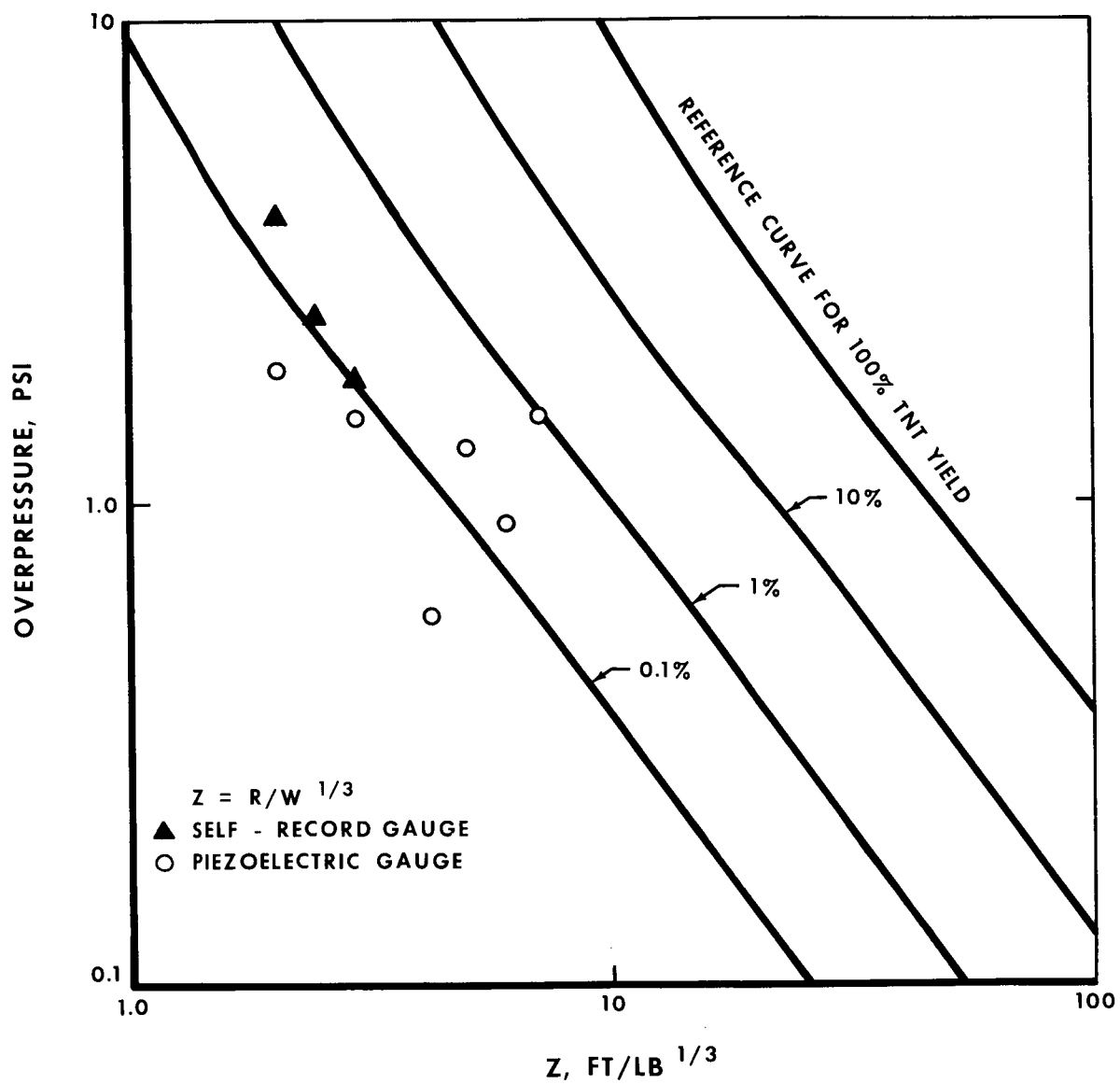


FIGURE 20 EQUIVALENT TNT YIELD FOR TEST C-2  
(EXTERNAL DESTRUCT SYSTEM)

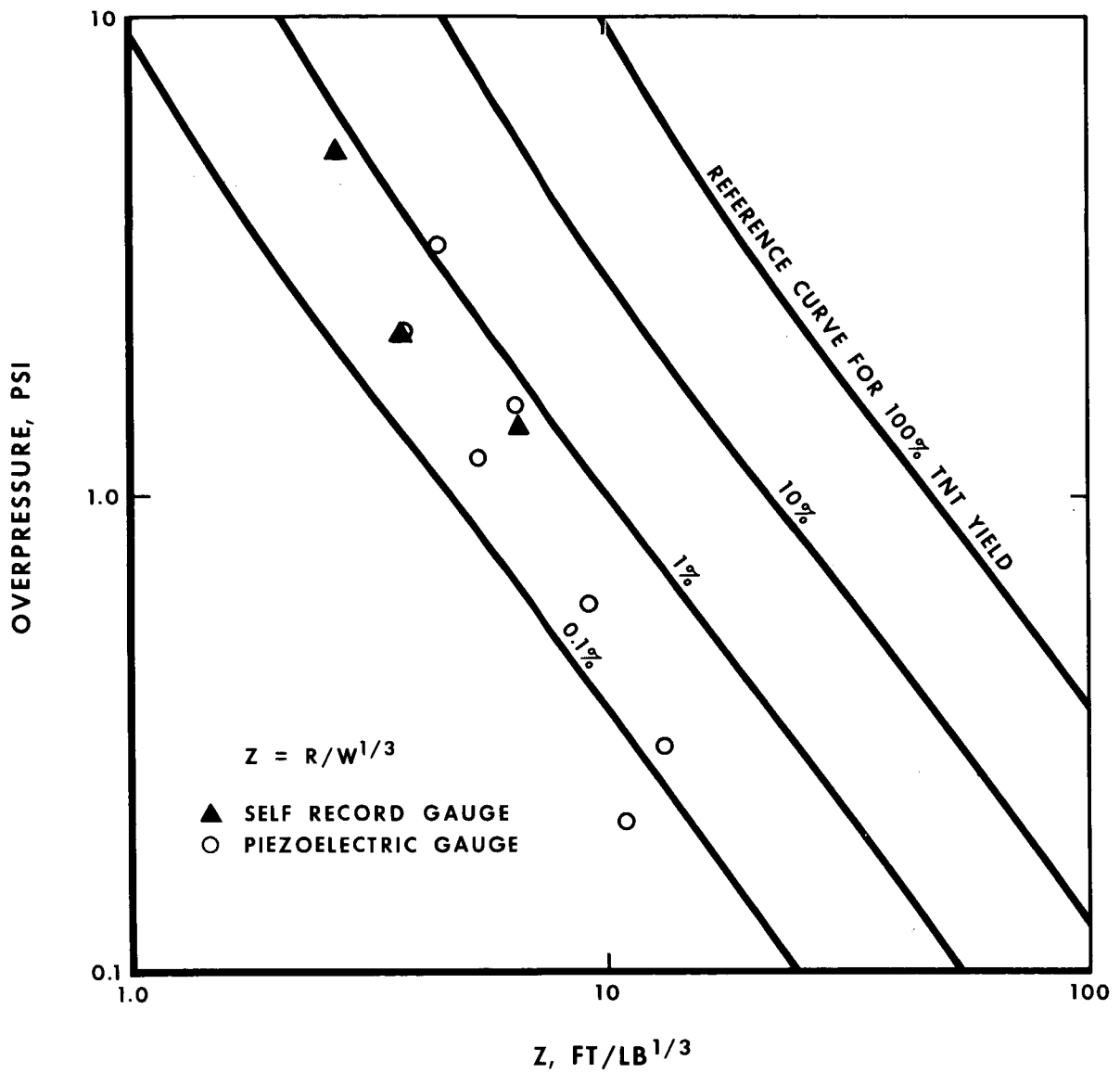


FIGURE 21 EQUIVALENT TNT YIELD FOR TEST C-3  
(INTERNAL DESTRUCT SYSTEM)

## REFERENCES

1. Baker, W. E., Ewing, W. O., Jr., Hanna, J. W., Bunnewith, G. E., "The Elastic and Plastic Response of Cantilevers to Air Blast Loading," BRL Report No. 1121. December 1960
2. "Blast Evaluation of Bare and Cased High Explosives," National Northern Report, NN-P-30. July 1955.
3. Ewing, W. O. and Hanna, J. W., "A Cantilever for Measuring Air Blast," BRL Technical Note 1139. August 1957.
4. Reisler, R. E., "The Mechanical Self-Recording Pressure-Time Gauge," DOD Bulletin No. 28, Part III, page 99, Shock, Vibration and Associated Environments.

February 3, 1964

APPROVAL

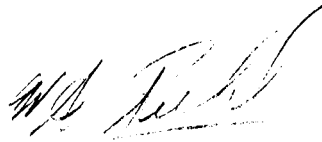
TM X-53007

DESTRUCT TESTS ON SCALE MODEL SATURN I BOOSTER

By

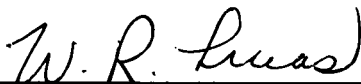
J. B. Gayle and C. H. Blakewood

The information in this report has been reviewed for security classification. Review of any information concerning Department of Defense or Atomic Energy Commission programs has been made by the MSFC Security Classification Officer. This report, in its entirety, has been determined to be unclassified.



---

W. A. Riehl  
Chief, Chemistry Branch



---

W. R. Lucas  
Chief, Materials Division



---

W. A. Mrazek  
Director, Propulsion and Vehicle Engineering Laboratory

# DISTRIBUTION

DIR	Dr. von Braun
DEP-T	Dr. Rees
R-DIR	Mr. Weidner
KN-DIR	Dr. Debus
KN-LA	Mr. Gorman
KN-S	Mr. King
KN-FS	Mr. Body
KN-LP	Mr. Thomas
LVO-DIR	Dr. Gruene
LVO-AD	Mr. Zeiler
R-AERO-DIR	Dr. Geissler
R-ASTR-E	Mr. Fichtner
I-I/IB-DIR	Col. L. James
I-V-SII	Mr. Cox
R-P&VE-DIR	Dr. Mrazek
R-P&VE-M	Dr. Lucas (5)
R-P&VE-MCP	Dr. Gayle (25)
R-P&VE-MC	Mr. Riehl
R-P&VE-ME	Mr. Kingsbury
R-P&VE-MM	Mr. Cataldo
R-P&VE-MN	Mr. Shannon
R-P&VE-P	Mr. Paul
R-P&VE-PE	Mr. Head
R-P&VE-PE	Mr. Bergeler
R-P&VE-PE	Mr. Rudder (5)
R-P&VE-PM	Mr. Voss
R-P&VE-PPS	Mr. Eilerman
R-P&VE-S	Mr. Kroll
R-P&VE-SDB	Mr. Wilhold
R-P&VE-SL	Mr. Showers
R-P&VE-V	Mr. Palaoro
R-P&VE-VI	Mr. Faulkner
R-P&VE-VK	Mr. Barraza
R-P&VE-VN	Mr. Thrower
R-P&VE-VO	Mr. Kistler
R-P&VE-VS	Mr. Schulze
R-P&VE-VSA	Mr. Beck
R-P&VE-VSA	Mr. Prasthofer
R-P&VE-N	Mr. Keller
R-TEST-DIR	Mr. Heimbarg
R-TEST-M	Mr. Dyer
R-TEST-T	Mr. Driscoll
R-TEST-T	Mr. Johnston
MS-F	Mr. Roberts
R-P&VE-RT	Mr. Hofues
MS-H	Mr. Akens
MS-IP	Mr. Remer
MS-IPL	Miss Robertson (8)
CC-P	Mr. Wofford

DISTRIBUTION (Concluded)

NASA Headquarters  
Washington, D. C. 20546  
Attn: Capt. R. F. Freitag, Dir. Launch Veh & Prop, OMSF  
Mr. G. D. McCauley, NASA Safety Office  
Mr. R. A. Schmidt, MLO

NASA-Manned Spacecraft Center  
Houston, Texas 77001  
Attn: Mr. R. F. Fletcher

NASA-Western Operations Office  
Technical Division  
150 Pico Boulevard  
Santa Monica, California 90404  
Attn: Mr. R. M. Mueller

Atlantic Missile Range  
Headquarters, Air Force Missile Test Center  
Patrick Air Force Base, Florida  
Attn: Mr. L. J. Ullian, MTORS-3

Air Force Rocket Propulsion Laboratory  
Air Force Systems Command  
Edwards Air Force Base, California  
Attn: Mr. C. R. Cooke, RPRX (3 copies)

Army Missile Support Command  
Explosives Division  
Redstone Arsenal, Alabama  
Attn: Mr. J. D. Maples

Space Nuclear Propulsion Office  
Cleveland Extension  
National Aeronautics and Space Administration  
Cleveland, Ohio 44135  
Attn: Mr. P. M. Ordin

Armed Services Explosives Safety Board  
Washington 25, D. C.  
Attn: Mr. R. C. Herman

Scientific & Technical Information Facility  
Attn: NASA Representative  
(S-AK/RKT)  
P. O. Box 5700  
Bethesda, Maryland